An Experimental Investigation of the Neural Correlates of the Acquired Capability for Suicide

by

John Zachary Willis

A thesis submitted to the Graduate Faculty of
Auburn University
in partial fulfillment of the
requirements for the Degree of
Master of Science

Auburn, Alabama
August 5, 2017

Keywords: Functional MRI, Gender differences in Suicide, Emotion Regulation, Risk Taking, Fearlessness of Death, Pain Tolerance

Approved by

Gopikrishna Deshpande, Chair, Associate Professor, Electrical & Computer Engineering
Thomas S Denney, Director, Auburn University MRI Research Center
Jeffrey S. Katz, Professor, Department of Psychology

Abstract

The high rate of fatal suicide attempts in men is a pressing issue as highlighted in the public conscious. The interpersonal–psychological theory of suicide has offered an explanation for the difference in suicidal behavior between men and women, suggesting that the desire to attempt suicide has separate constructs from the ability to commit suicide. In order for an individual to have suicidal desire and the acquired capability for suicide, in order to commit suicide. Higher levels of the acquired capability for suicide would explain the higher rate of fatal suicide attempts among men. In this study, we have attempted to analyze several constructs identified as possibly underlying the neural substrates involved in the acquired capability for suicide. Additionally, we compared the results of males and females in the hope of identifying possible regions that lead to the higher number of fatal suicides in men. The constructs analyzed were pain tolerance, emotional stoicism, fearlessness about death, and sensation seeking. Participants were asked to complete tasks designed to model theses constructs. Parametric modulation was used to better identify neural regions of interest. A group consisting of all male participants was compared against a group consisting of all female participants. In this comparison, we found that the premotor cortex and the cerebellum, regions which are involved in motor function, had significantly higher activation in males than females. This may support the higher rate of suicides in males over females. Future studies should perform this analysis in individuals in the population of interest and use a larger sample size.

Acknowledgments

I would like to express my gratitude to my parents for their support throughout my life and academic pursuits.

I would like to thank my advisor Dr. Gopikrishna Deshpande, for supporting me throughout my undergraduate and graduate studies. I am grateful to him for his support and advice all through the thesis research.

I would like to thank Dr. Tracy Witte for her role in this research. Her expertise and prior research in this field is what got this project started. I would also like to thank Dr. Thomas Denney and Dr. Jeffrey Katz for agreeing to serve on my graduate committee and review my thesis work.

Table of Contents

List of Tables

List of Figures

List of Abbreviations

MRI	Magnetic Resonance Imaging
fMRI	functional Magnetic Resonance Imaging
IPTS	Interpersonal–Psychological Theory of Suicide
ACS	Acquired Capability for Suicide
ACSS	Acquired Capability for Suicide Scale
ACSS-FAD	Acquired Capability for Suicide Scale – Fearlessness About Death
BART	Balloon Analog Risk Task

Chapter 1: Introduction

1.1 MRI

Magnetic Resonance Imaging (MRI) is a technique for observing the anatomy and physiology of the body using powerful magnets. It is commonly used for the diagnoses of medical conditions. MRI observes out body by influencing the large number of hydrogen nuclei (single protons) in our body. Under everyday circumstances, the protons are randomly aligned, each spinning around an arbitrary axis. These arbitrary positions result in a net zero magnetic field. A large magnetic field, B0, is applied to the body by a MRI scanner affects the hydrogen protons (fig. 1.1 A). Many protons in the body began to align themselves with the magnetic field (parallel) and a few against the field (anti-parallel) (fig. 1.1 B), and all hydrogens begin to precess about the field (fig. 1.1 C). This leads to the body having a net magnetization in the direction of the magnetic field. A magnetic pulse, B1, occurring at the Larmor frequency, which is calculated based on the proton being influenced and the strength of B0, is applied by RF coils in a direction perpendicular to B0. After a period of time, this pulse flips the spins of the protons from the longitudinal plane into the transverse plane, towards the coil. When the RF pulse is switched off, the spins return to the longitudinal plane, either parallel or anti-parallel to field B0, over the recovery time, T1. Also, at the same time, the spins are dephasing from each other due interference from other protons, this is known as transverse relaxation. This occurs over the relaxation time, T2. Some protons decay faster due to local inhomogeneity in the magnetic field. This is known as free induction decay with the time constant T2* (fig. 1.1 D). The signal, which is strongest after the RF pulse is switched off, quickly decays due to longitudinal decay and

transverse relaxation. To counteract the decay in the signal due to dephasing, another RF pulse is applied that flips the spins 180°. After a time, TE, the spins again overlap resulting in the spin-echo. Three gradient coils cause differences in the magnetic fields in the body across their respective directions. This allows for unique field strengths in the three-dimensional space of the body. This causes protons throughout the body to spin at different rates, which allows us to obtain spatial information of the body. Cycling the RF pulse through the range of frequencies across all the magnetic field gradients in a magnetic field, we can obtain a three-dimensional volume of the entire tissue. This provides 3D images without using known harmful radiations. The data of a magnetic resonance image is stored in an array of numbers known as the k-space. The intensity of the signal stored in the k-space is dependent on the relaxation times, T1 and T2, and the proton density. Different tissues of the body have different relaxation times and proton densities, which results in contrasts between the tissues in the final image. Each cell in k-space contains information about every pixel of the image. The center rows of k-space contain base of the image contrast, and the outer rows contain the fine details. A Fourier transform of the k-space gives the magnetic resonance image [1]–[4].

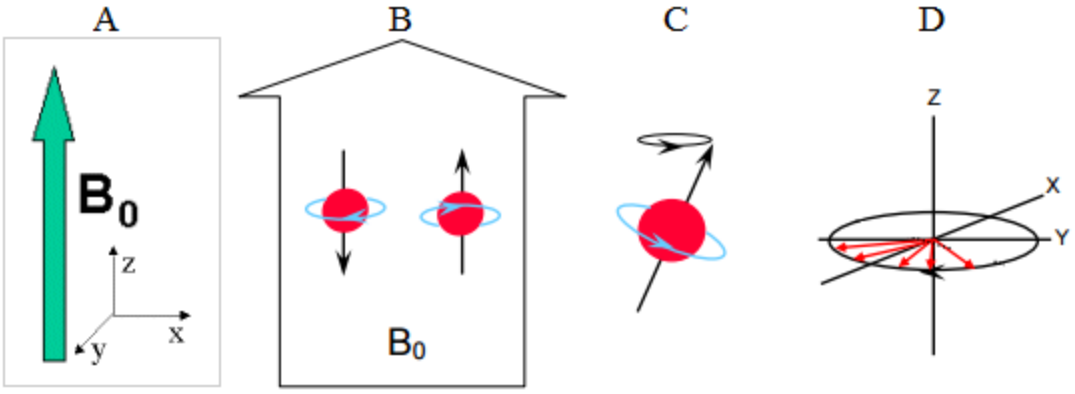

Figure 1.1 A*. Magnetic field B0 applied during fmri.* ***B****. Protons aligned parallel or anti-parallel to the magnetic field.* ***C****. In the presence of B0, protons precess about the field.* ***D****. After removing the RF pulse, spins dephase at different rates. This results in around the "clock face" [3], [4].*

1.2 fMRI

Functional Magnetic Resonance Imaging (fMRI) is a technique that utilizes MRI to investigate brain activity over time [5]. A pulse sequence called echo-planar imaging (EPI) rapidly changes the gradient coils of MRI machine. EPI acquires all rows of the k-space in a single repetition. This allows us to collect data from the brain over small time intervals. fMRI is an indirect measurement of neural activity as it is based on the blood oxygenation level dependent (BOLD) contrast. This relies on the difference in magnetization between de-oxygenated blood, which is paramagnetic compared to the surrounding tissue, and oxygenated blood, which is more diamagnetic than water. Activity in a region of the brain increase metabolic demand in that region, which increases the blood flow to that region to supply oxygen. This results in an increase of oxygenated blood arriving at the region a few seconds after the neuronal activity and a decrease in the amount of de-oxygenated blood in that region. This change in oxygenation creates distortions in the magnetic field in the blood and the surrounding extra-

vascular area. The protons in these regions are affected by these field distortions, which affects the signal decay process, characterized by T2 (spin echo) or T2* (gradient echo) decay [6]. MRI detects these distortions and represents it as image intensity in the MRI scans. The change in MR signal, the hemodynamic response, appears 1 to 2 seconds after neuronal activity and peaks around 5 seconds after activity. The BOLD response can be modelled by convolving the hemodynamic response with the series of impulses representing neuronal activity [7]. fMRI has a high spatial resolution on the order of millimeters, but has a poor temporal resolution of 1 to 2 seconds. Combining fMRI with electroencephalography (EEG) or magnetoencephalography (MEG) allows for the spatial resolution of fMRI and the high temporal resolution of EEG/MEG. The spatial resolution of fMRI makes it beneficial for both research and clinical applications.

1.3 Interpersonal–Psychological Theory of Suicide

The interpersonal–psychological theory of suicide (IPTS) is a proposed explanation on the constructs that lead to suicidal behavior. It suggests that thwarted belongingness and perceived burdensomeness are necessary for a person to desire to engage in suicide. An addition to the IPTS, known as the acquired capability for suicide (ACS) seeks to outline the constructs that lead to persons engaging in suicidal behavior. These are pain tolerance and fearlessness about death. Additionally, two other constructs have been identified as possible contributors to ACS, emotional stoicism and sensation seeking [8]–[10].

1.4 Pain Tolerance

Pain Tolerance has been a subject of interest in research involving fMRI. Previous studies of pain tolerance used either electrical stimulation of thermal stimulation to induce pain in participants. Davis et al. designed a device using a sphygmomanometer that would induce physical pain in participants [11]. The device is to be used by steadily increasing the pressure at a set rate. The pressure would be released when the participant signaled for it or when the pressure reached the limit of what is deemed safe. This device should allow for stimulation that more closely resembles pain experienced in everyday situations.

1.5 Emotion Regulation

Suppression of emotion and other forms of arousal has been a subject of many studies. The International Affective Picture System (IAPS) [12] provides a useful resource for images that can be used in these studies. From the IAPS, pictures of the desired emotion and neutral pictures can be chosen. By showing the pictures to participants in the MRI machine and having given them instructions on how they should decrease or increase arousal from the pictures, neural activity underlying emotion stoicism can be studied.

1.6 Fearlessness About Death

One of the constructs examined by the Acquired Capability for Suicide Scale (ACSS), based on constructs delineated by Joiner [9], is fearlessness about death. Fear regarding death is not a commonly studied subject, and, unlike other constructs examined by the ACSS, lacks a task designed to observe its neural substrates. As such, a questionnaire focusing solely on the

fearlessness about death aspect of the ACSS was devised as to study fearless about death isolated from other forms of fear and constructs in the ACSS (see Ribeiro et al. [13]). This revised ACSS contains questions that are rated by the subject on a scale, e.g. from 1-4 with 1 being “not at all like me” and 4 being “very much like me.” There are also reversed questions in the questionnaire, e.g. if a standard question is “I am very much afraid to die” then a reversed question would be “I am not at all afraid to die.” By isolating fearlessness about death, its contribution to the ACS can be examined.

1.7 Balloon Analog Risk Task

The Balloon Analog Risk Task (BART) is a task designed by Lejuez et al. [14] to examine risk taking, a form of sensation seeking. BART involves presenting a virtual balloon via screen to participants. Participants can inflate the balloon to maximize virtual currency. At any point, they can stop inflating the balloon to “bank” their winnings. Each inflation of the balloon increases the chance for the balloon to pop, by which all currency for that balloon is lost. Participants are encouraged to maximize their virtual winnings in an allotted time. There is also a version of BART in which all results are randomly determined and participants provide no input, which serves as a control.

1.8 General Linear Model

The general linear model (GLM) is a way to explain the variation of a known, dependent variable in terms of a linear combination of reference functions (fig 1.2). The dependent variable is the observed fMRI time course of a voxel. The reference functions, also known as

regressors, are based on experimental conditions or nuisance parameters, like motion parameters. Regressors are multiplied by an estimate, or weight, of the regressors effect on the dependent variable. Anything not included in the regressors is part of the error [15].

$$
\begin{aligned}
y_1 &= b_0 + b_1 X_{11} + \cdots \cdots \cdots + b_p X_{1p} + e_1 \\
y_2 &= b_0 + b_1 X_{21} + \cdots \cdots \cdots + b_p X_{2p} + e_2 \\
y_3 &= b_0 + b_1 X_{31} + \cdots \cdots \cdots + b_p X_{3p} + e_3 \\
&\vdots \qquad\qquad\qquad\quad \vdots \qquad\quad \vdots \qquad \vdots \\
y_n &= b_0 + b_1 X_{n1} + \cdots \cdots \cdots + b_p X_{np} + e_n
\end{aligned}
$$

Figure 1.2 A system of equations for voxel time course y with n data points. X represents regressors, b represents weights, and e represents error [15].

1.9 Organization of Thesis

fMRI is a MRI-based neuroimaging technology that allows for non-invasive mapping of brain activity at a spatial resolution in the order of millimeters. This makes it a useful tool in detecting functional activation in the brain; allowing for better understanding of human cognitive functions.

The aim for this thesis is to utilize fMRI to perform a study to investigate the relationship between gender and suicidal behavior, particularly fatal behavior. Participants performed four tasks that mimicked characteristics identified in the interpersonal–psychological theory of suicide (IPTS) and the acquired capability for suicide (ACS). Task were analyzed individually to ensure their accuracy. Additionally, each task was analyzed with regressors to emphasize results that mimicked the characteristics being researched. The tasks were combined together as to

compare male against female participants. This would allow for us to observe any differences that may explain the difference between fatal suicide behavior and gender.

Chapter 2: An Experimental Investigation of the Neural Correlates of the Acquired Capability for Suicide.

Abstract

The high rate of fatal suicide attempts in men is a pressing issue as highlighted in the public conscious. The interpersonal–psychological theory of suicide has offered an explanation for the difference in suicidal behavior between men and women, suggesting that the desire to attempt suicide has separate constructs from the ability to commit suicide. In order for an individual to have suicidal desire and the acquired capability for suicide, in order to commit suicide. Higher levels of the acquired capability for suicide would explain the higher rate of fatal suicide attempts among men. In this study, we have attempted to analyze several constructs identified as possibly underlying the neural substrates involved in the acquired capability for suicide. Additionally, we compared the results of males and females in the hope of identifying possible regions that lead to the higher number of fatal suicides in men. The constructs analyzed were pain tolerance, emotional stoicism, fearlessness about death, and sensation seeking. Participants were asked to complete tasks designed to model theses constructs. Parametric modulation was used to better identify neural regions of interest. A group consisting of all male participants was compared against a group consisting of all female participants. In this comparison, we found that the premotor cortex and the cerebellum, regions which are involved in motor function, had significantly higher activation in males than females. This may support the higher rate of suicides in males over females. Future studies should perform this analysis in individuals in the population of interest and use a larger sample size.

2.1 Introduction.

Over 40,000 people commit suicide every year in the United States [16]. Non-fatal suicide attempts are estimated to occur at 25 times the rate of fatal suicide attempts [16]. One of the well-established findings in the epidemiology of suicide is that men are more likely to die by suicide than women [17]. This occurs even though men are less likely to experience depression [e.g. Piccinelli et al and Van de Velde et al ([18], [19])], suicidal ideation [20], and non-fatal suicide attempts [20]. Part of this can be attributed to men choosing more lethal methods [21], [22]; however, accounting for those who choose the same method, men are more likely to have a fatal suicide attempt than women [23].

One possible theory for this difference is the interpersonal–psychological theory of suicide (IPTS) [[8], [9]]. According to the IPTS, fearlessness about death and tolerance of pain are needed to make a lethal suicide attempt. Joiner [9] combined these two concepts into a construct known as the acquired capability for suicide (ACS). The IPTS suggests that men are more likely than women to obtain the acquired capability for suicide, a proposition that has come up in behavioral literature [e.g. [10], [13], [24], [25]]. There are two main explanations by the IPTS for why men have higher ACS. First, ACS is acquired though life experiences that are painful and provocative. Many of these experiences (e.g., combat exposure, impulsive/aggressive behaviors) are more common among men. Second, there is the possibility that various neurobiological and temperamental factors give an individual a higher chance to acquire the capability for suicide [8]. A study by Witte et al. [10]examined sensation seeking and emotional stoicism as potential characteristics that explain the relationship between gender and ACS. Across two independent samples, sensation-seeking fully accounted for the

relationship between gender and fearlessness about death, and stoicism fully accounted for the relationship between gender and physical pain tolerance. These characteristics provide a theoretical and psychological framework for exploring the neural correlates of the observed gender differences in the ACS.

Deshpande et al. studied the neural substrates underlying the gender differences in suicidal behavior. In that study, they performed a meta-analysis using activation likelihood estimation using papers from the BrainMap database. In order to obtain a large sample of experiments, Deshpande et al. approximated the constructs of ACS to some key words: Emotional stoicism to emotion, pain tolerance to pain, fearlessness of death to fear, and sensation-seeking to experiments with paradigm class involving reward. Their analysis found that men experience notable activation in premotor, primary motor, and cerebellar regions in the studies of interest [26]. This may support the fact that suicidal desires lead to more fatal attempts in males than females.

The meta-analysis is useful in generating a hypothesis, but lacks precise modelling of the constructs of ACS. This study aims to test the results of Deshpande et al. by using actual experimental data obtained from four tasks of interest: Fear regarding death, pain tolerance, emotional regulation (emotional stoicism), and risk taking (sensation seeking).

2.2 Methods

A. Participants

Nine healthy individuals (5 male, 4 female; 77.7% Caucasian) participated in this study. Participants were between 19 and 26 years old (Mean = 21; Standard deviation = 2.1) and right-

handed. The experimental protocol was approved by the Auburn University Institutional Review Board and the experiment was conducted in compliance with internationally accepted ethical standards. All participants reported no history of neurological or sensory disorders, fainting, seizure, or current use of cigarettes or pain medication. All participants provided informed consent and were screened for MRI exclusionary criteria in accordance with protocols approved by the Institutional Review Board. Subjects received $40 as compensation for their participation.

B. Tasks

After consent and briefing, participants changed into MRI-safe surgical scrubs. Prior to entering the scanning room, participants received verbal instruction from a researcher about the tasks they were expected to perform inside the scanner. Participants were given the opportunity to practice the Emotion Regulation Task (ERT) and the Balloon Analogue Risk Task (BART) outside the scanner in order to ensure that they understood the procedure. The images used for practicing the ERT were separate from the images used in the actual trial. Each participant performed four tasks inside the scanner in the following order and will be described below: 1) pain tolerance, 2) emotion regulation, 3) fearlessness about death, and 4) risk taking (Figs. 2.1, 2.2, 2.3, and 2.4, respectively).

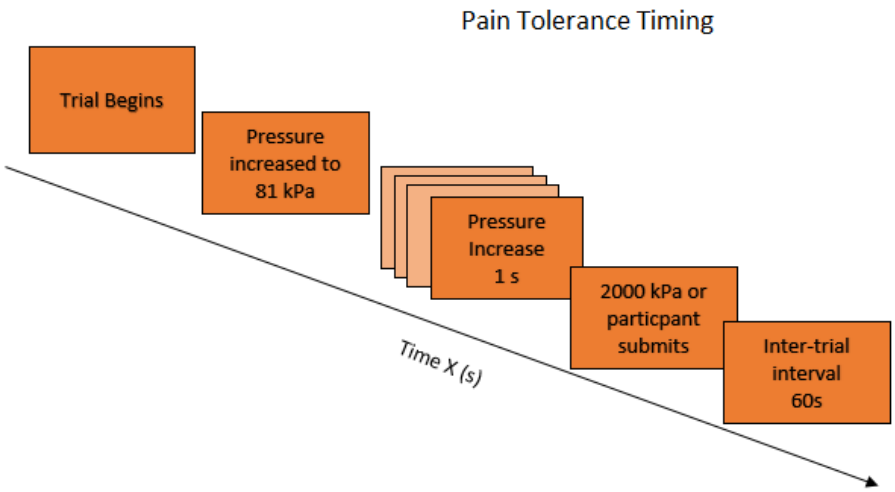

Figure 2.3 Timing of Pain Tolerance Task

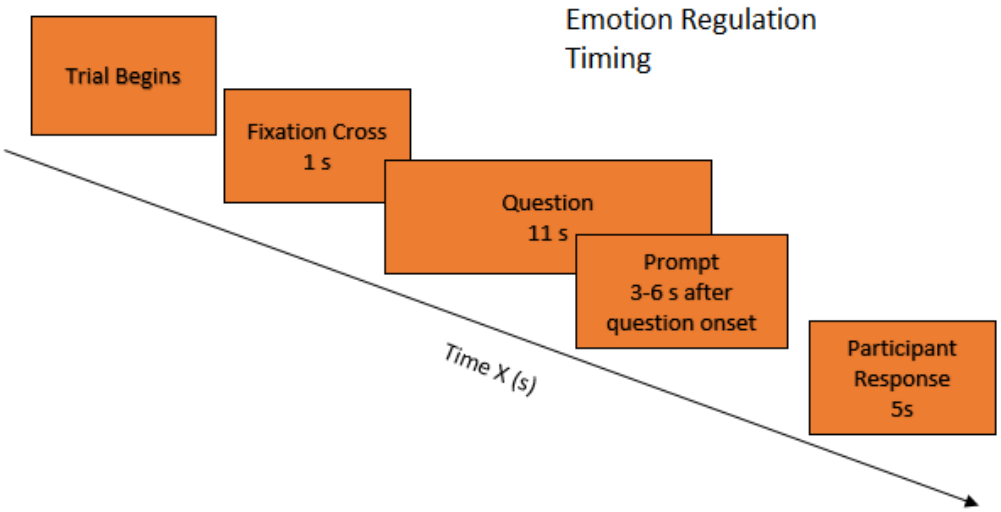

Figure 2.4 Timing of Emotion Regulation Task

Pain tolerance was measured by applying pressure in increasing amounts to the participants' right hand using a MRI safe device described in Davis et al. [11]. The device was attached to the

participants' right hand while they were in a supine position. Participants were asked to observe a white cross that was

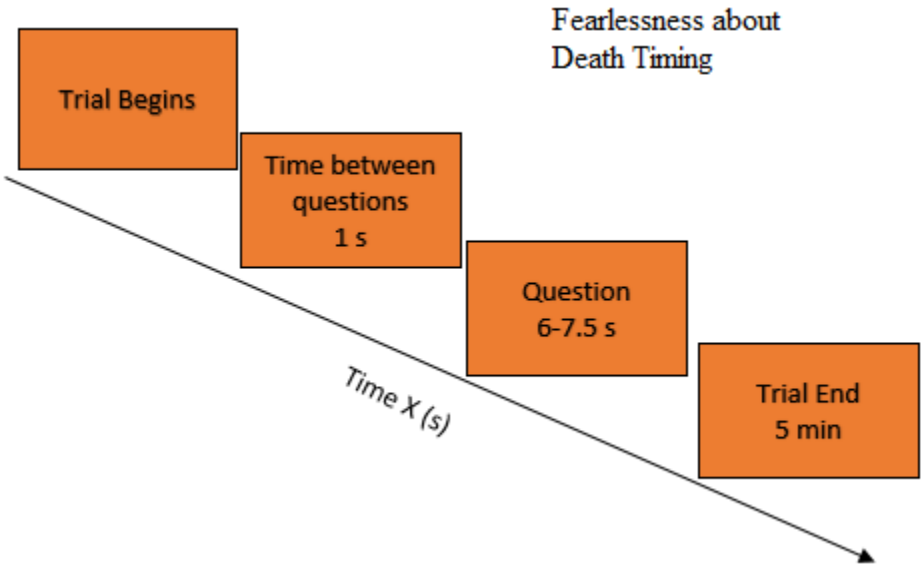

Figure 2.5 Timing of Fearlessness About Death Task

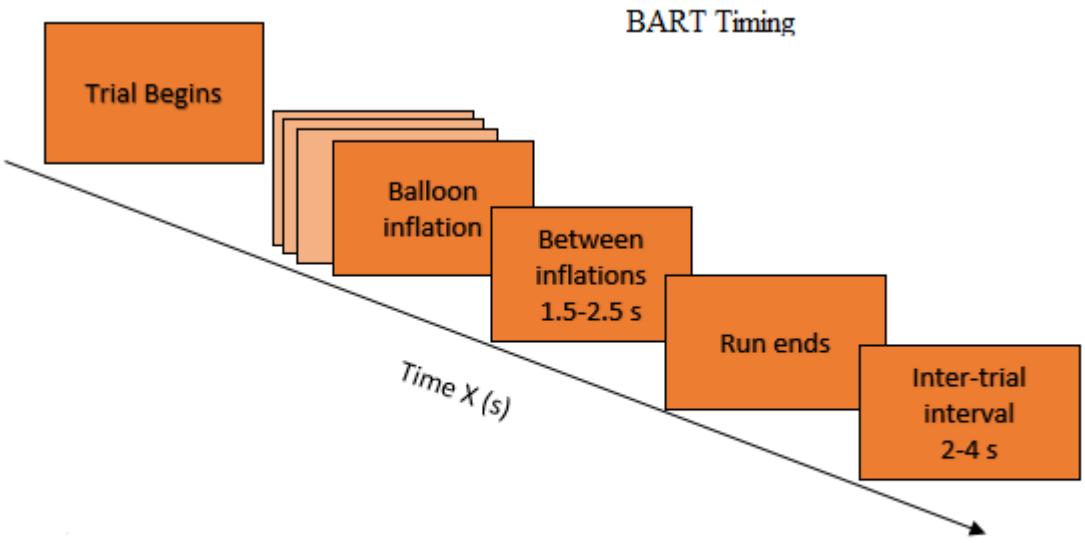

Figure 2.6 Timing of BART Task

projected on to a screen inside the scanning bore. This cross was observable via a mirror affixed to the participants' head coil. Pressure was administered by a researcher in the MRI control room. The vinyl tubing of the pressure device ran through a howl in the wall normally reserved for fiber optic cable. Timing was controlled and recorded with a custom-made program in E-Prime (v. 2.0; Psychological Software Tools, Pittsburgh, PA).

The pressure was increased to 81 kPa [11] prior to each trial. During the trial, the pressure was increased by squeezing a bulb once every second. Pressure was released over an inter-trial interval of 60 s (Fig.1). This sequence occurred 10 times. For each trial, pressure was immediately released when the participant signaled that the pain was too uncomfortable using any button on an infrared 4-button controller. If a participant did not signal by 2000 kPa, the trial was immediately ended based on safety standards in literature [27].

The task design for emotion regulation was adopted from Urry et al [28]. Prior to the task, participants received visual instructions regarding the task. Subjects were asked that upon receiving the cue "increase" to either 1) imagine the event occurring to themselves or a loved one, or 2) imagine a more extreme outcome to the current image. Upon receiving the cue "decrease," subjects were asked to either 1) view the depicted situation as fake, or 2) imagine a positive outcome to the situation being depicted. For the "maintain" cue participants were instructed to maintain their attention to the picture.

Participants were shown of series of images taken from the International Affective Picture System [12], 36 of the images were highly arousing (1, least arousing to 9, most arousing; 5.82±0.80) and negative (1, most unpleasant to 9, most pleasant; 2.35±0.57) and 12 images were neutral, i.e. not arousing (3.14±0.79), pleasant or unpleasant (5.04±0.29). The task was divided

into two blocks of 24 images (18 negative and 6 neutral). Negative images showed disturbing events, animals and people. The neutral images were everyday objects. Images were preceded by a white fixation cross for 1 s, before being displayed for 11 s. All negative images were paired with cue words to either decrease, increase, or maintain their emotional response and neutral images were paired with only the maintain cue. These cues appeared 3, 4, 5, or 6 s after picture onset (Fig. 2.2). Stimulus presentation was pseudorandomized to prevent consecutive presentation of more than three trials of the same condition. After each stimulus, participants were given 5 s to self-rate the success of emotion regulation on a four-point scale (1, no emotion; 2, not at all successful; 3, somewhat successful; and 4, very successful).

The fearlessness about death task is based on the Acquired Capability for Suicide Scale-Fearlessness about Death (ACSS-FAD). In this task, participants were instructed to respond to an ACSS-FAD questionnaire (Fig. 2.5) with 42 questions. There have been several studies assessing the usefulness of the ACSS in examining fearlessness about death (e.g. Ribeiro et al., Witte et al., and Spangenberg et al. [13], [14], [20]. But there has been no study examining the ACSS-FAD in the fMRI context to the best of our knowledge. Each question appeared on screen for either 6, 6.5, 7, or 7.5 s, chosen at random, and there was 1 s between the end of one question and the start of the next (Fig. 2.3). Participants responded to the questions on a 4-point scale (“1” - not at all like me, “4” – very much like me).

BART from Rao et al.[30] was used to assess the neural correlates of risk-taking. In the BART, participants were presented with an image of a balloon in the center of the screen. They were instructed to click the button labeled “start” to begin inflating the balloon. Each press of “start” would inflate the balloon, and with each inflation, a “virtual reward” would accumulate

in a temporary bank. At any point, participants could stop pumping the balloon by pressing the button labeled “Collect $$$.” This would transfer the reward from the temporary bank into a permanent bank labeled “Total Earned.” Each inflation of the balloon posed a larger risk of the balloon exploding, which results in all money in the temporary bank being lost and no effect on the permanent bank. Participants were instructed to maximize the total reward. To incentivize the participants to perform well, they were told prior to the scan that their results on this task would be compared to other participants and if they are in the bottom 33%, they will earn an extra $1, the middle 33% will earn an extra $5, and the top 33% will earn an extra $10.

ACSS-FAD

Please read each item below and indicate to what extent you feel the statement describes you.

	Not at all like me 1	2	3	Very much like me 4
1. The fact that I am going to die does not affect me.	○	○	○	○
2. The pain involved in dying frightens me.	○	○	○	○
3. I am very much afraid to die.	○	○	○	○
4. It does not make me nervous when people talk about death.	○	○	○	○
5. The prospect of my own death arouses anxiety in me.	○	○	○	○
6. I am not disturbed by death being the end of life as I know it.	○	○	○	○
7. I am not at all afraid to die.	○	○	○	○
8. Death is no doubt a grim experience.	○	○	○	○
9. I avoid death thoughts at all costs.	○	○	○	○
10. I am disturbed by the finality of death.	○	○	○	○
11. Whenever the thought of death enters my mind, I try to push it away.	○	○	○	○
12. I always try not to think about death.	○	○	○	○
13. I have an intense fear of death.	○	○	○	○
14. I avoid thinking about death altogether.	○	○	○	○
15. The fact that death will mean the end of everything as I know it frightens me.	○	○	○	○
16. I try to have nothing to do with the subject of death.	○	○	○	○
17. The uncertainty of not knowing what happens after death worries me.	○	○	○	○
18. I am afraid of dying very slowly.	○	○	○	○
19. I am afraid of dying in a fire.	○	○	○	○
20. I am afraid of experiencing a great deal of pain when I die.	○	○	○	○
21. I am afraid of dying of cancer.	○	○	○	○
22. I have a fear of suffocating (including drowning).	○	○	○	○
23. I have a fear of dying violently.	○	○	○	○
24. The thought that my dying could be long and painful is unbearable.	○	○	○	○
25. I am frightened by the idea that all my thoughts and feelings will stop when I am dead.	○	○	○	○
26. Inwardly, I resist the thought of my own death.	○	○	○	○
27. I feel fear at the very idea of dying slowly and in agony someday.	○	○	○	○
28. Thinking beyond the threshold of my death makes me feel afraid.	○	○	○	○
29. The physical decline that accompanies a slow dying process disturbs me.	○	○	○	○
30. The very idea that my entire personality will disappear forever with my death appalls me.	○	○	○	○
31. The idea that I will never be able to think and experience anything after my death disturbs me.	○	○	○	○
32. I am afraid of dying a painful death one day.	○	○	○	○
33. I am afraid of being treated as a mere object when I lie dying.	○	○	○	○

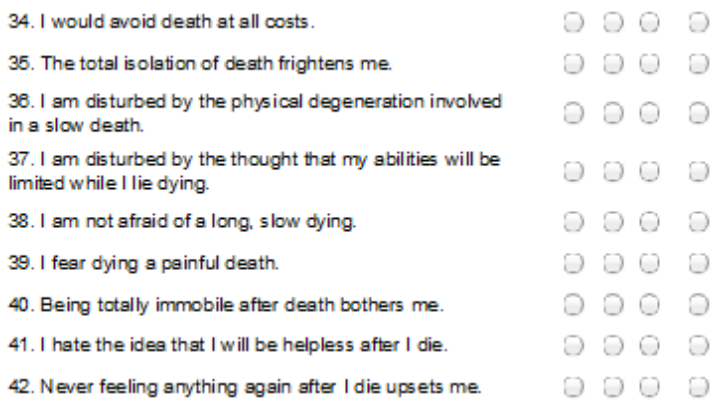

Figure 2.7 ACSS-FAD Questionnaire

All participants were, in fact, told that they scored in the top 33% after the scan and were given the $10. In the passive version of the trial, participants were instructed to simply press the button when prompted. The result of each press of the button was decided by the computer. The passive task was identical to the active task in all other aspects.

Both the active and passive BART tasks lasted a total of 6 minutes each, which meant that participants varied in the number of balloons completed. Participants were cued to press a button when a small circle on the screen changed from red to green. After each inflation of the balloon, the circle turned red for 1.5-2.5 s, before turning green, signaling that the participant could then inflate the balloon again. After the result of one balloon, there was a 2-4 s inter-trial interval before the next balloon began (Fig. 2.4).

A safety squeeze bulb was taped to the participants' chest that, when squeezed, would alert the researchers to stop all scanning immediately.

C. Data acquisition

Functional and anatomical data were acquired using a 7T Siemens (Erlangen, Germany) MAGNETOM scanner equipped with a Nova 32-channel head coil (Nova Medical, Wilmington,

MA). Each participant's anatomical data were collected with an individual 3D, T1-weighted magnetization prepared rapid gradient-echo (MP-RAGE) image [31]with the following parameters: field of view (FOV) = 215 × 215 × 192 mm^3, matrix = 256 × 256 × 160, voxel size = 0.84 × 0.84 × 1.2 mm^3, TR (repetition time) = 1900 ms, TE (echo time) = 2.75 ms, TI (inversion time) = 1050 ms, flip angle = 7°, bandwidth = 240 Hz/pix, averages = 1. Functional images were collected using gradient echo, multiband echo planar imaging (EPI) [32]with the following parameters: TR = 1000 ms, TE = 20 ms, flip angle = 70°, voxel size = 2 × 2 × 2 mm^3 with whole brain coverage, and multiband factor = 2.

D. Data Preprocessing

Statistical Parametric Mapping 12 (SPM12, The Wellcome Trust Centre for Neuroimaging, Institute of Neurology, University College London), was used for preprocessing and analysis of all data. Preprocessing steps included realignment, co-registration, normalization to Montreal Neurological Institute (MNI) space, denoising of time series using low and high pass filters and spatial smoothing. Realignment (i.e., motion correction) was performed with a 6 degrees of freedom (3 translation and 3 rotation) rigid body registration which minimized the error in a least squares sense. Images with head movement above 0.5 mm were excluded and replaced with images derived using cubic spline temporal interpolation to ensure continuous temporal data for all subjects. All mean functional images created during realignment were co-registered with high resolution anatomical images obtained during MP-RAGE, and all remaining functional images were re-sliced to align with this reference image. Spatial normalization was used to nonlinearly warp all participants' brains to the MNI template image.

To increase the signal-to-noise ratio after realignment and normalization, data were smoothed using a Gaussian kernel with a full-width half-maximum of $8 \times 8 \times 8$ mm^3.

E. Activation analysis.

We examined parametric increases of the BOLD signal with pressure (pain tolerance), BOLD response during suppression of negative emotional response (emotion regulation), evoked response to questions related to fearlessness of death (fearlessness about death), and the BOLD response to risk-taking (BART) in voxels across the brain using a random-effects general linear model (GLM). This involved building GLMs at the individual subject level (first-level) with regressors corresponding to the main effects of the desired response for each task, as well as the parametric effect of increasing pressure or risk. Nuisance regressors based on six head motion parameters and derivatives of the hemodynamic response function for modeling its variability were also used.

First-level analysis was done on a per-subject, per-task basis. For pain tolerance, the regressors were parametrically modulated such that higher pressure trials were given more weight, corresponding to the amount of pain the participants were in.

Emotion regulation consisted of the following trials according to picture type and prompt: negative-maintain, negative-suppress, negative-enhance, or neutral-maintain. Relevant contrasts consisted of enhance>maintain and suppress and suppress>maintain and enhance. These contrasts were chosen in order to compare our results to previous studies. Emotion regulation trials were parametrically modulated using the trial specific responses from the participants. Responses of “1” were given minimal weight in the parametric analysis, as those response

indicated no self-reported success in emotion regulation from the participant. Responses of “2,” “3,”and “4” increased the parametric weight respectively.

In the first level analysis for fearlessness of death the regressors were parametrically weighted using the participant responses (on a scale of 1-4) about how fearless they felt about death.

BART trials were separated based on the results: win, loss, or inflate. Loss and inflate were the trials of interest as those signaled continued risk taking. As such, the design matrix was constructed so that TRs corresponding to loss and inflate were set to “1”, win was set to “-1” and others were set to “0”. The parametric modulation applied to the task was based on the risk level. Each inflation increases the risk and, thus, increases the weight given to it.

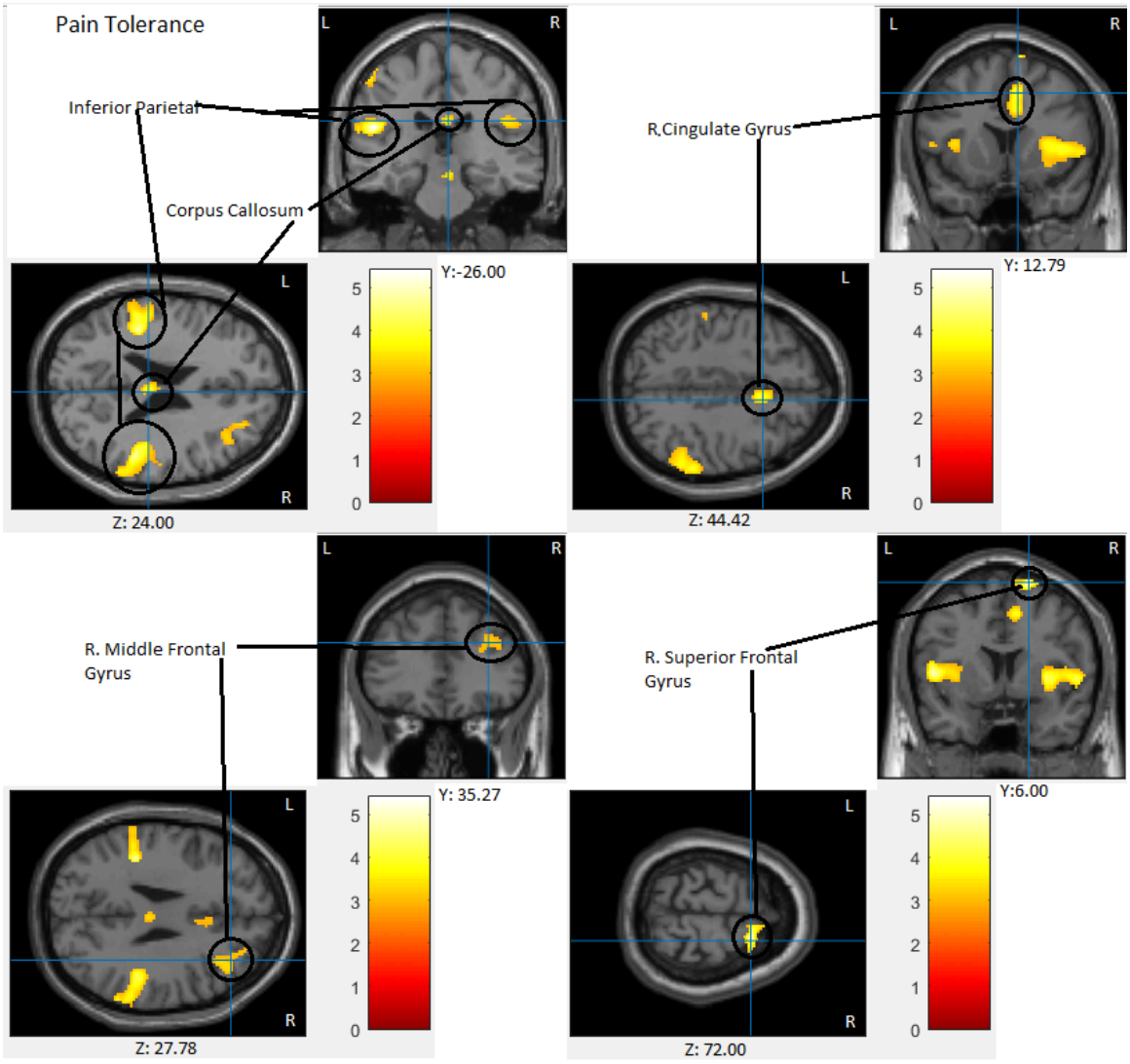
Pain Tolerance
Inferior Parietal
Corpus Callosum
L
R
Y:-26.00
Z: 24.00
5
4
3
2
1
0
R.Cingulate Gyrus
Y: 12.79
Z: 44.42
R. Middle Frontal Gyrus
Y: 35.27
Z: 27.78
R. Superior Frontal Gyrus
Y:6.00
Z: 72.00

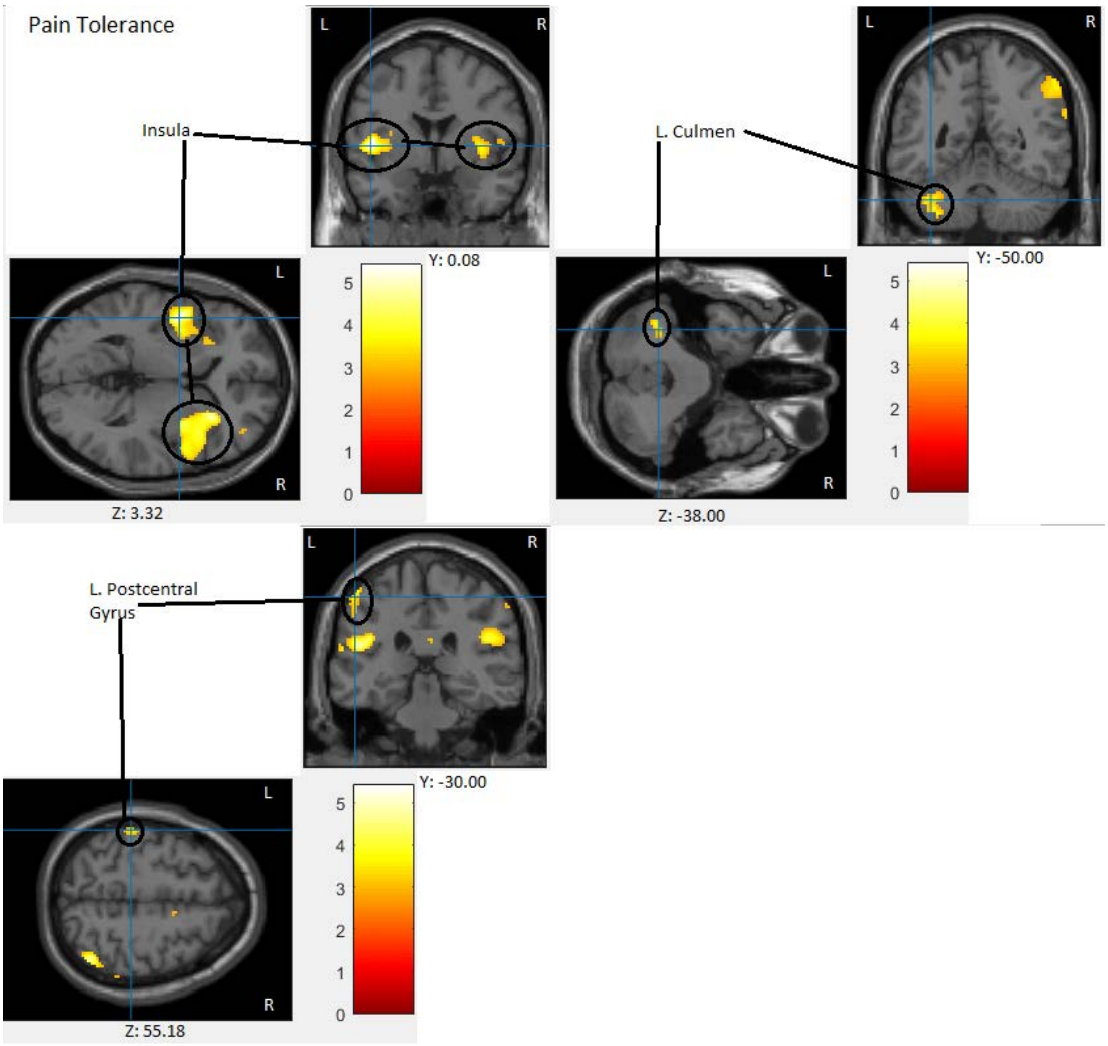

Figure 2.8 The BOLD fMRI activation map for Pain Tolerance task.

The results of the first-level analysis were then entered into second-level analyses. First, for all the tasks, the contrast maps obtained from individual subjects were used to perform second-level t-tests in order to confirm the validity of our results with previous literature. Next, contrast maps obtained from male participants were compared with those obtained from female participants across all tasks using a two sample t-test. This was done in order to determine

gender-specific differences across the four constructs of ACS. We preferred this approach over gender-specific contrasts for each task since our sample size was small and the adopted approach increased our degrees of freedom by collating contrast maps from all task for each gender.

2.3 Results

Major activation areas ($p<0.01$, corrected with cluster size >= 25) for pain tolerance can be found in Figure 2.6. Table 2.1 gives information on clusters. Notable areas of activation are bilaterally in the insula, bilaterally in the inferior parietal, corpus callosum, and right cingulate.

Emotion regulation (enhance>maintain and suppress) shows bilateral deactivation in the temporal gyrus, occipital gyrus and cuneus as well as deactivation in the left frontal gyrus. There are also small areas of activation in the right cerebellum and bilaterally in the precuneus/calcarine. These regions are shown in Figure 2.7 ($p<0.01$, corrected with cluster size >= 25 for enhance>maintain and suppress; $p<0.05$, corrected with cluster size >= 100 for suppress>maintain and enhance. Here a different threshold was used for better comparison with previous results) and clusters are shown in Table 2.2. Deactivations for suppress>maintain and enhance are seen bilaterally in the insula and occipital, lingual, and

Table 2.1 Table of clusters for the Pain Tolerance task

Region	BA	x	y	z	Peak intensity	Cluster Size (voxels)
R. Insula	13, 47	28	24	0	5.15	1507
R. Inf. Parietal	40	54	-38	22	4.81	1374
L. Inf. Parietal	40	-40	-34	26	5.31	602
L. Insula, L. Precentral	22, 44	-46	0	6	5.41	589
R. Cingulate, R. Supp. Motor Area	24, 32	10	8	48	4.08	470
R. Frontal	9	26	42	18	3.43	341
L. Cerebellum	*	-36	-50	-38	3.87	263
R. Sup. Frontal	6	20	6	72	5.08	96
L. Insula	13	-26	22	8	3.51	92
L. Postcentral	2	-50	-30	60	3.61	86
R. Corpus Callosum	23	4	-26	24	3.87	66
R. Frontal	10	42	46	0	3.44	49
L. Cerebellum Post.	*	-20	-66	-50	3.51	29

frontal gyri. The left superior temporal gyrus deactivates, while the right superior and middle portions of the temporal gyrus activate (Fig. 2.8 and table 2.3). Additionally, the right superior temporal gyrus and left cerebellum deactivate.

Fearlessness about death showed deactivation throughout the brain at the regular threshold ($p<0.01$, corrected with cluster size >= 25). The threshold was adjusted ($p<0.000002$, corrected with cluster size>= 25) to obtain clusters of activation which are shown in Figure 2.9 and Table 2.4. To obtain a better understanding of how fearlessness of death relates to suicide, we paired the results of pain tolerance against fearlessness of death. This gives us regions that are shared by pain tolerance and fearlessness of death, which may give us a better understanding of how they relate to each other and to suicide. The regions shared by these tasks are the bilateral insula and right inferior frontal gyrus and are seen in Figure 2.10 and table 2.5.

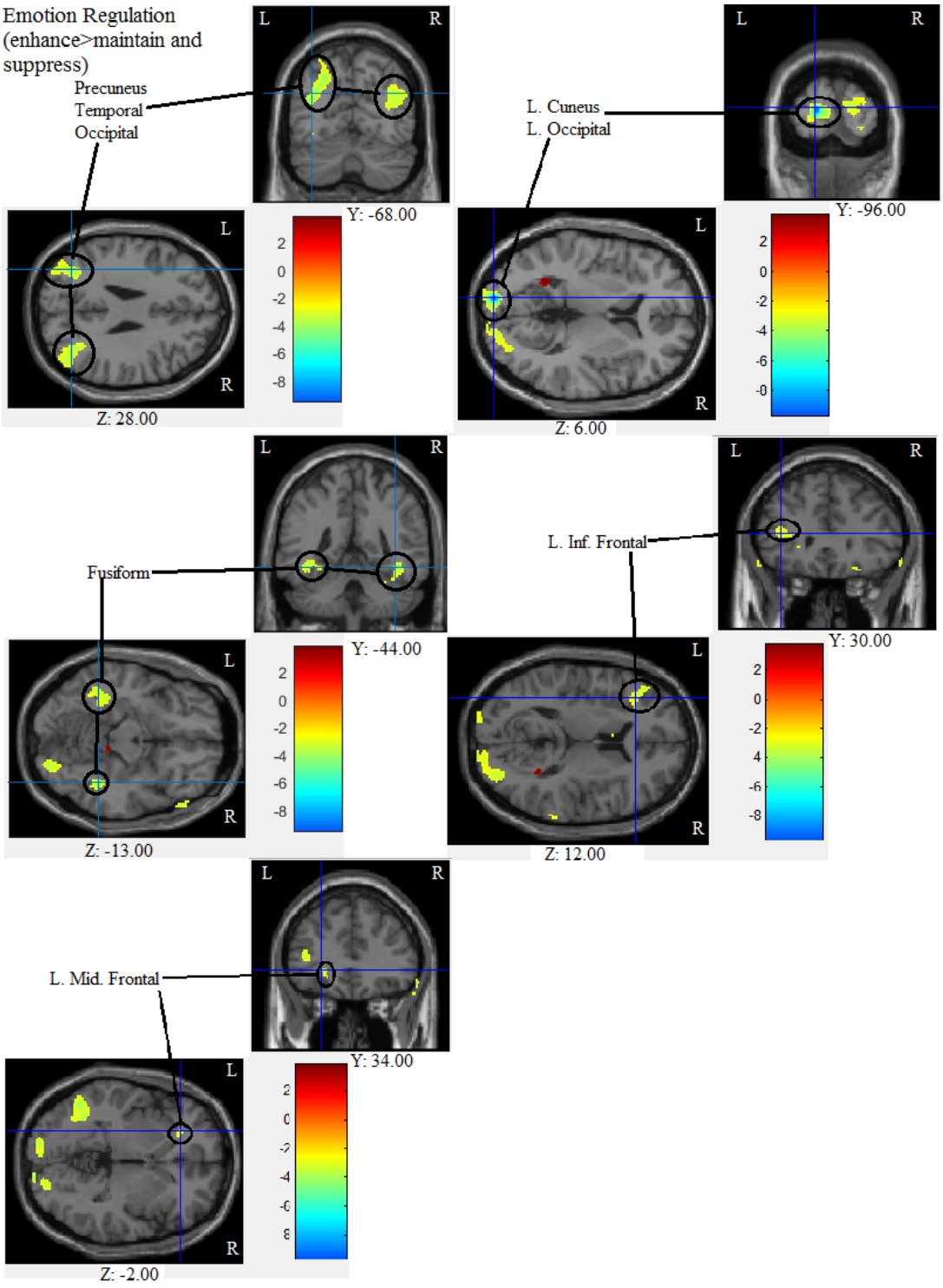

Figure 2.9 The BOLD fMRI deactivation map for Emotion regulation (enhance>maintain and suppress) task.

Table 2.2 Table of clusters for the Emotion Regulation (enhance>maintain and suppress) task

Region	BA	x	y	z	Peak intensity	Cluster Size (voxels)
R. Temporal, R. Occipital, R. Cuneus	18, 19, 39	42	-72	20	-4.43	1333
L. Occipital, Precuneus	7, 19, 39	-36	-66	24	-4.94	734
L. Temporal, L. Fusiform	37	-38	-42	-8	-5.10	554
L. Occipital, L. Cuneus	17, 18	-12	-96	6	-9.55	315
R. Fusiform	*	42	-44	-10	-4.88	173
L. Inf. Frontal	*	-46	40	12	-3.73	139
L. Inf. Frontal	*	-42	6	22	-3.50	43
L. Mid. Frontal	*	-24	34	-2	-3.34	34
L. Lateral Ventricle	*	-30	-52	8	3.80	32
R. Mid Temporal	*	62	-8	-6	-3.74	30
L. Precuneus, L. Calcarine	*	-30	-52	8	3.80	32
L. Supp. Motor Area	*	-10	14	48	-3.50	26
R. Cerebellum	*	10	-34	-16	3.60	26

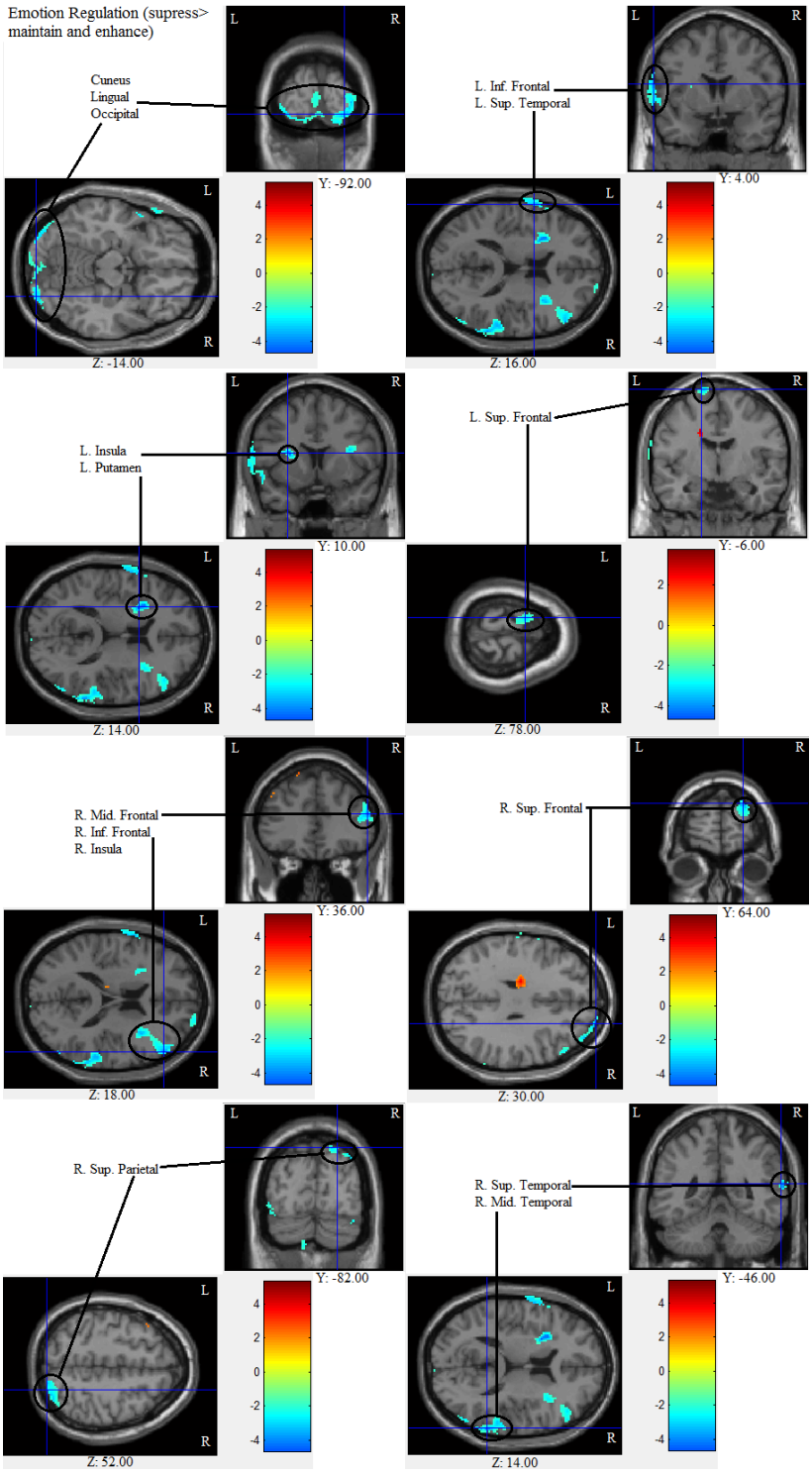

Figure 2.10 The BOLD fMRI deactivation map for Emotion regulation (suppress>maintain and enhance) task.

Table 2.3 Table of clusters for the Emotion Regulation (suppress>maintain and enhance)

Region	BA	x	y	z	Peak intensity	Cluster Size (voxels)
Mid. Occipital Gyrus, Inf. Occipital Gyrus, Lingual Gyrus, Cuneus	17, 18, 19	34	-96	0	-3.67	827
L. Inf, Frontal Gyrus, L. Sup. Temporal Gyrus	6, 22, 47	-64	4	16	-3.75	605
R. Mid. Frontal Gyrus, R. Inf. Frontal Gyrus, R. Insula	46	54	36	20	-4.05	514
R. Sup. Temporal Gyrus, R. Mid. Temporal Gyrus	14, 22	66	-46	14	-4.03	417
R. Sup. Parietal Lobule	7	18	-82	52	-3.26	268
L. Cerebellum, Uvula	*	-16	-70	-44	-3.68	211
R. Sup. Frontal Gyrus	10	24	64	30	-3.83	174
L. Insula, L. Putamen	*	-26	10	14	-4.58	147
L. Sup. Frontal Gyrus	6	-14	-6	78	-3.13	135
L. Cerebellum	18	-16	-74	-18	-3.69	116

BART showed deactivation in a large area of the brain. There is bilateral activation in the occipital gyrus, lingual gyrus, fusiform gyrus, caudate, and insula. Notable areas of activation can be found in Figure 2.11 ($p<0.01$, corrected with cluster size >= 25). Cluster information is in Table 2.6.

Fearlessness about Death

p<0.000002 for all of fearlessness about death

Angular_L (aal)
Sup. Temporal Gyrus

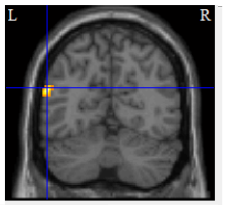

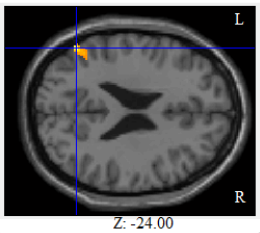

Y: -64.00

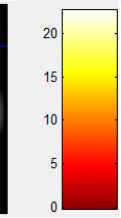

Z: -24.00

L. Cingulate Gyrus

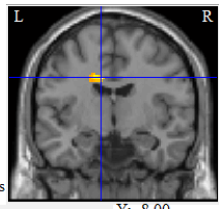

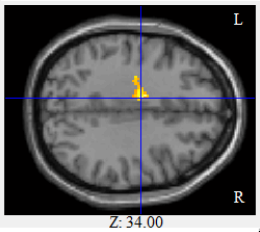

Y: -8.00

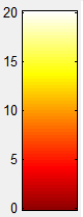

Z: 34.00

L. Mid. Frontal Lobe

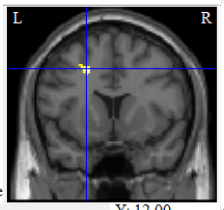

Y: 12.00

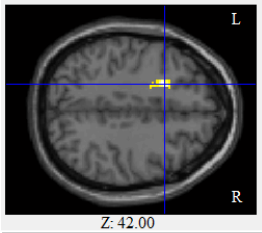

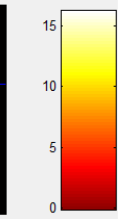

Z: 42.00

L. Mid. Temporal Gyrus
L. Sup. Temporal Gyrus
L. Putamen
L. Insula

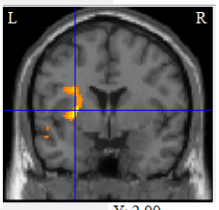

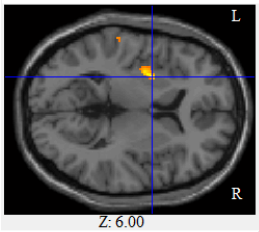

Y: 2.00

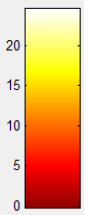

Z: 6.00

L. Parahippocampa Gyrus
L. Hippocampus
L. Fusiform Gyrus

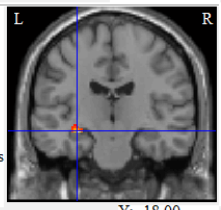

Y: -18.00

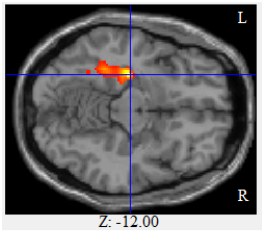

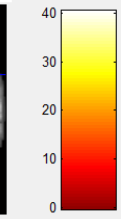

Z: -12.00

L. Sup. Occipital Gyrus
L. Cuneus
L. Mid. Occipital Gyrus

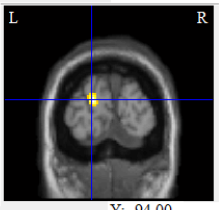

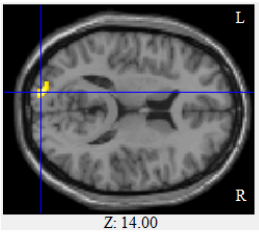

Y: -94.00

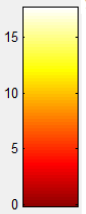

Z: 14.00

L. Sup. Temporal Gyrus
L. Trans. Temporal Gyrus

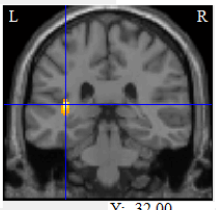

Y: -32.00

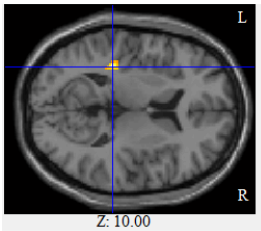

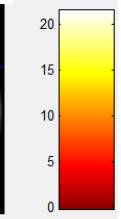

Z: 10.00

Med. Frontal Gyrus
Mid. Frontal Gyrus
Sup. Frontal Gyrus

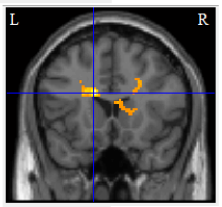

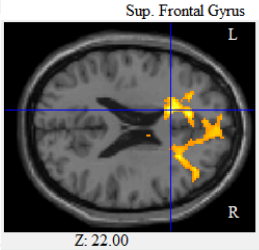

Y: 18.00

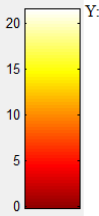

Z: 22.00

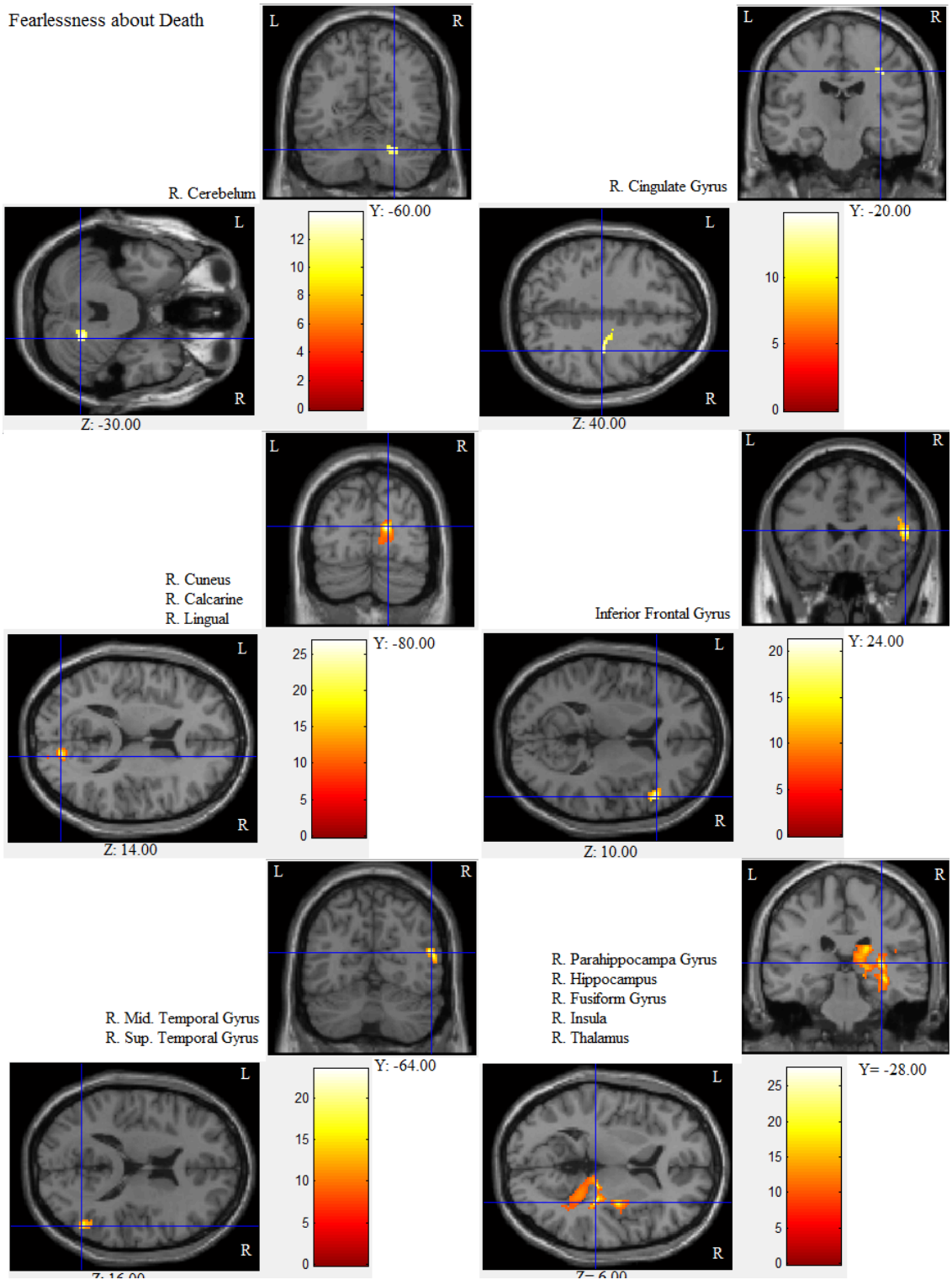

Figure 2.11 The BOLD fMRI deactivation map for Fearlessness About Death task.

Table 2.4 Table of Deactivations for Fearlessness of Death task

L. Mid. Temporal Gyrus, L. Sup. Temporal Gyrus, L. Putamen, L. Insula	21, 38	-28	2	6	-24.47	1078
L. Parahippocampa Gyrus, L. Hippocampus, L. Fusiform Gyrus	37	-30	-18	-12	-40.36	867
R. Cuneus, R. Calcarine, R. Lingual	18	16	-80	14	-26.79	368
R. Inf. Frontal Gyrus	45	52	24	10	-21.29	152
Angular_L (aal), L. Sup. Temporal Gyrus	39	-54	-64	24	-22.61	148
L. Sup. Temporal Gyrus, L. Trans. Temporal Gyrus	41	-36	-32	10	-21.48	122
R. Mid. Temporal Gyrus, R. Sup. Temporal Gyrus	39	52	-64	16	-23.47	115
R. Cingulate Gyrus	*	34	-20	40	-14.72	107
L. Cingulate Gyrus	*	-10	-8	34	-20.10	107
L. Sup. Occipital Gyrus, L. Cuneus, L. Mid. Occipital Gyrus	18	-14	-94	14	-17.66	106
R. Cerebelum	*	24	-60	-30	-13.79	103
L. Mid. Frontal Lobe	8	-22	12	42	-16.19	101

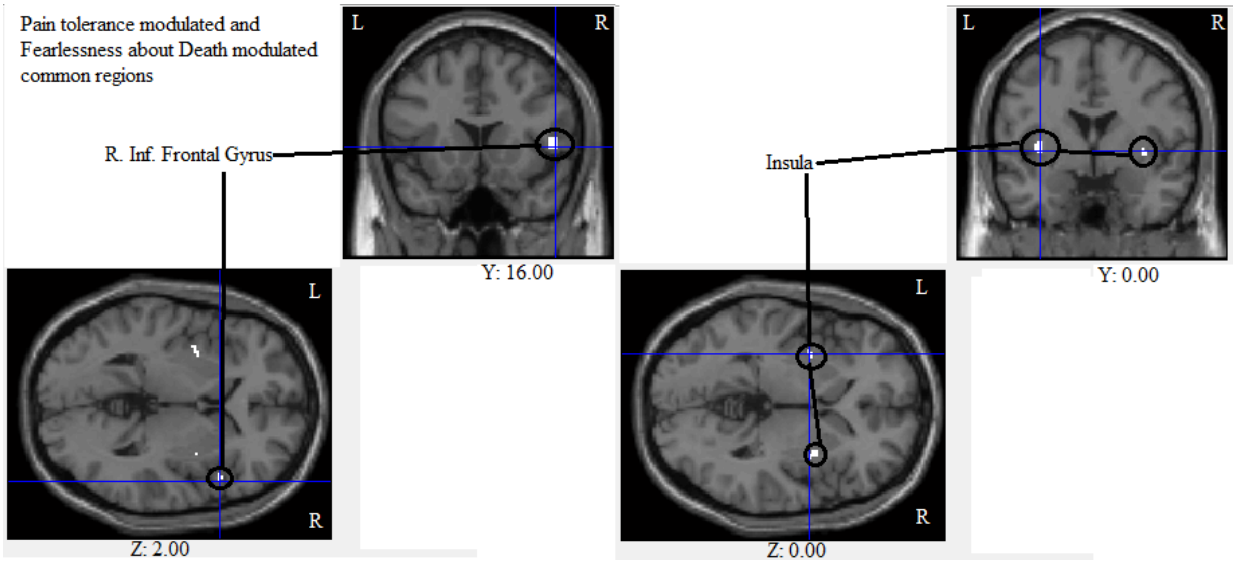

Figure 2.12 Overlap of activation maps for Pain Tolerance and Fearlessness about Death ((binary image).

Table 2.5 T able of major activations for Pain Tolerance>Fearlessness of Death

Region	x	y	z	Cluster Size (voxels)
R. Inf. Frontal	52	16	2	28
L. Insula	-34	0	0	22
R. Insula	34	2	-4	18

Comparing contrast maps obtained from male participants with those obtained from female participants across all tasks using a two sample t-test showed that the premotor cortex and cerebellum were significantly ($p<0.01$ corrected) more activated in males than in females, as seen in Figure 2.12. Exact cluster locations and intensities are shown in Table 2.7.

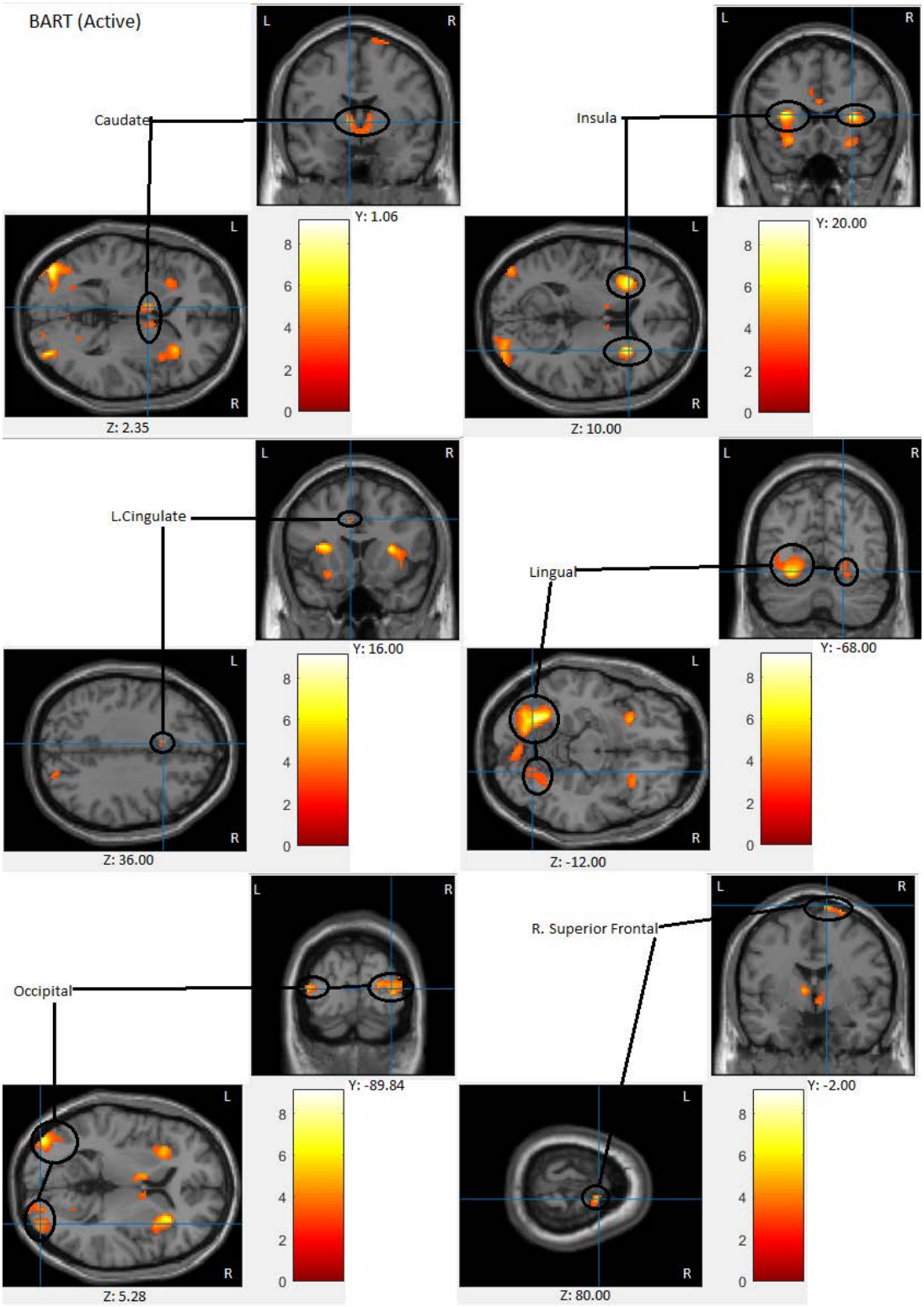

Figure 2.13 The BOLD fMRI activation map for BART task.

Table 2.6 Table of clusters for the BART task

Region	BA	x	y	z	Peak intensity	Cluster Size (voxels)
L. Occipital, L. Lingual, L. Fusiform	18, 19	-26	-64	-10	9.09	1629
R. Insula, R. Frontal	13, 47	30	20	10	8.37	468
L. Insula, L. Frontal	13, 47	-32	20	10	7.40	446
L. Mid. Occipital	18, 19	34	-88	0	7.45	341
Caudate	*	-8	-2	4	4.90	231
R. Occipital, R. Lingual, R. Fusiform	18, 19	20	-68	-12	3.61	193
R. Sup Frontal	6	12	-2	80	5.49	121
R. Sup Occipital, R. Precuneus	*	22	-76	32	5.57	87
L. Cingulate	32	-6	16	36	4.07	72
L. Frontal	*	-34	56	26	3.50	38

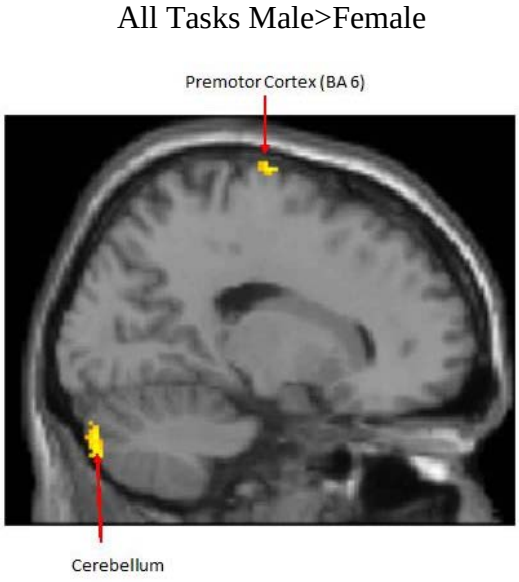

Figure 2.14 The BOLD fMRI activation map for Male>Female in all tasks

Table 2.7 Table of clusters for Male>Female in all tasks

Region	BA	x	y	z	Peak intensity	Cluster Size (voxels)
Premotor Cortex	6	18	-14	80	3.2149	27
Cerebellum	*	16	-88	-36	3.9319	225

2.4 Discussion

Davis et al. [11] compared the results of the pain tolerance device used here with those reported in previous pain tolerance papers. They showed that our pressure pain device showed results similar to those obtained using electrical and thermal pain devices.

Looking at the results from emotion regulation (enhance>maintain and suppress), we found deactivation in the fusiform gyrus, occipital gyrus, temporal gyrus, cuneus, and left frontal gyrus. This is very similar to the results from Urry et al., Table 1. One of the key similarities is the lack of right frontal gyrus activation and smaller activation in the right fusiform compared to the left. Unfortunately, Urry et al. lacks a similar table for suppress>maintain and enhance. As such, a similar paper, Harenski et al. [33] had to be used to compare the results. Our results show deactivation bilaterally throughout the frontal, occipital and temporal gyri. This matches with the locations given in Tables 3 and 4 in Harenski et al.

Comparing our results to Rao et al. [30], we see much of the same activations as seen in Table 2 of Rao et al. In particular, activity that involves a large portion of the midbrain, including the insula, and thalamus, and extending into the frontal cortex. Other areas of activation include the caudate/striatum, fusiform, and occipital regions.

An overlap of regions activated by pain tolerance and deactivated by fearlessness of death showed only bilateral insula. This means that the insula increased activation with pain tolerance

and decreased activation with fearlessness of death. This shows the centrality of insula to processing death related information in the context of suicidal ideation and planning. This is consistent with a previous study by Shi and Han [34] which showed activation in the insula while processing death related linguistic cues.

With the validity of our individual tasks confirmed, we can then proceed to examine gender differences. Across all tasks, male participants showed higher activation in the premotor cortex and cerebellum as compared to females. The premotor cortex is involved in planning motor movements prior to the movement being performed. The cerebellum is involved in a number of movement related processes, including motor planning [35], [36]. Although all tasks involved button presses, related activations must cancel out both at the first- and second-level analyses because both the conditions and subject samples would have button-press related activations. Further, even though the tasks had motor-related components, they were subtracted out in the contrasts used. These facts indicate that activity in these motor-related regions were higher in males compared to females while engaging in processes defined by the ACS. This suggests that, when males are engaging in processes involving Acquired Capability for Suicide constructs there is a sub-threshold and/or non-time locked response in two regions involved in motor planning. This activation may pre-dispose males towards action and could lead to fatal suicide attempts in those that are contemplating suicide.

A couple of limitations of this study are noteworthy. First, this study was performed on a group of healthy individuals. In order to verify the results, future studies will need to use participants from the population of interest, i.e. individuals susceptible to committing suicide. Second, the current study and associated findings are preliminary in nature given the rather

small sample size we have. Future studies must employ larger sample sizes in order to detect effects with greater statistical significance and control for false positives in a more conservative fashion.

Chapter 3: Conclusion

The aim of this thesis was to investigate the neural differences between males and females in four constructs identified by the acquired capability for suicide. The four constructs are as follows: pain tolerance, emotional stoicism, fearlessness about death, and sensation seeking. Emotional stoicism and sensation seeking were investigated through emotional regulation and risk taking, respectively. With suicide becoming an increasing issue in society, and a large gap between males and females in successful suicide attempts; there became a need to identify neural substrates involved in fatal suicide. To this end, Deshpande et al. [26] performed a meta-analysis based on the four constructs to identify possible substrates. The goal of this thesis was to test the results of the meta-analysis using tasks that model the constructs of interest. To accomplish this, previous literature similar to our constructs were investigated as to identify possible tasks. For pain tolerance, steadily increasing physical pain by using an sphygmomanometer was the chosen task. Suppression of negative emotions induced by pictures was used to model emotional stoicism. Fearlessness about death was modelled using a questionnaire designed to measure that particular construct. Finally, sensation seeking was modelled by using a task designed for risk taking via virtual gambling. These tasks were performed by each subjects in a single session. Comparing the results between males and females gave us results that matched those found by Deshpande et al.

Bibliography

[1] "Blink E. 'An easy introduction to Basic MRI Physics for anyone who does not have a degree in physics.' http://www.mri-physics.net/ (http://www.mri-physics.net/), 2004." .

[2] "Yoshioka H, Schlechtweg P and Kose K. 'Magnetic Resonance Imaging.' In Imaging of Arthritis and Metabolic Bone Disease, by Weissman BNW, 34-47. Philadelphia, PA: Mosby/Elsevier, 2009." .

[3] S. C. B. S. F. FACMP, *Magnetic Resonance Imaging: Physical and Biological Principles, 3e*, 3 edition. St. Louis, Mo: Mosby, 2003.

[4] "What is MRI? - University of Hull." [Online]. Available: http://www2.hull.ac.uk/science/mri/whatismri.aspx. [Accessed: 20-Jun-2017].

[5] S. A. Huettel, A. W. Song, and G. McCarthy, *Functional Magnetic Resonance Imaging, Second Edition*, 2nd edition. Sunderland, Mass: Sinauer Associates, 2008.

[6] K. R. Thulborn, J. C. Waterton, P. M. Matthews, and G. K. Radda, "Oxygenation dependence of the transverse relaxation time of water protons in whole blood at high field," *Biochim. Biophys. Acta*, vol. 714, no. 2, pp. 265–270, Feb. 1982.

[7] S. Ogawa, T. M. Lee, A. R. Kay, and D. W. Tank, "Brain magnetic resonance imaging with contrast dependent on blood oxygenation.," *Proc Natl Acad Sci U S A*, vol. 87, no. 24, pp. 9868–9872, Dec. 1990.

[8] K. A. Van Orden, T. K. Witte, K. C. Cukrowicz, S. R. Braithwaite, E. A. Selby, and T. E. Joiner, "The interpersonal theory of suicide.," *Psychological Review*, vol. 117, no. 2, pp. 575–600, 2010.

[9] T. Joiner, *Why People Die by Suicide*, 1 edition. Cambridge, Mass.: Harvard University Press, 2007.

[10] T. K. Witte, K. H. Gordon, P. N. Smith, and K. A. Van Orden, "Stoicism and sensation seeking: Male vulnerabilities for the acquired capability for suicide," *Journal of Research in Personality*, vol. 46, no. 4, pp. 384–392, Aug. 2012.

[11] M. T. Davis *et al.*, "Demonstration and validation of a new pressure-based MRI-safe pain tolerance device," *Journal of Neuroscience Methods*, vol. 271, pp. 160–168, Sep. 2016.

[12] "Center for the Study of Emotion and Attention (1999) The International Affective Picture System: digitized photographs. Gainesville, FL: Center for Research in Psychophysiology, University of Florida." .

[13] J. D. Ribeiro *et al.*, "Fearlessness about Death: The psychometric properties and construct validity of the revision to the Acquired Capability for Suicide Scale," *Psychol Assess*, vol. 26, no. 1, pp. 115–126, Mar. 2014.

[14] C. W. Lejuez *et al.*, "Evaluation of a behavioral measure of risk taking: The Balloon Analogue Risk Task (BART)," *Journal of Experimental Psychology: Applied*, vol. 8, no. 2, pp. 75–84, Jun. 2002.

[15] "The General Linear Model (GLM)." [Online]. Available: http://www.brainvoyager.com/bvqx/doc/UsersGuide/StatisticalAnalysis/TheGeneralLinearModel.html. [Accessed: 20-Jun-2017].

[16] “Drapeau CW, McINtosh JL. U.S.A. Suicide 2012: Official Final Data. Washington, DC: American Association of Suicidology (2014). Available from: www.suicidology.org.” .
[17] “World Health Organization. Suicide Rates per 100,000 by Country, Year, and Sex. (2011). Available from: www.who.int/mental_health/prevention /suicide_rates/en/index.html.” .
[18] M. Piccinelli, “Gender differences in depression: Critical review,” *The British Journal of Psychiatry*, vol. 177, no. 6, pp. 486–492, Dec. 2000.
[19] S. Van de Velde, P. Bracke, and K. Levecque, “Gender differences in depression in 23 European countries. Cross-national variation in the gender gap in depression,” *Social Science & Medicine*, vol. 71, no. 2, pp. 305–313, Jul. 2010.
[20] M. K. Nock *et al.*, “Cross-national prevalence and risk factors for suicidal ideation, plans and attempts,” *The British Journal of Psychiatry*, vol. 192, no. 2, pp. 98–105, Feb. 2008.
[21] K. Hawton, “Sex and suicide: Gender differences in suicidal behaviour,” *The British Journal of Psychiatry*, vol. 177, no. 6, pp. 484–485, Dec. 2000.
[22] D. L. Schrijvers, J. Bollen, and B. G. C. Sabbe, “The gender paradox in suicidal behavior and its impact on the suicidal process,” *Journal of Affective Disorders*, vol. 138, no. 1–2, pp. 19–26, Apr. 2012.
[23] A. Cibis *et al.*, “Preference of lethal methods is not the only cause for higher suicide rates in males,” *J Affect Disord*, vol. 136, no. 1–2, pp. 9–16, Jan. 2012.
[24] M. J. Cambron, L. K. Acitelli, and J. W. Pettit, “Explaining Gender Differences in Depression: an Interpersonal Contingent Self-Esteem Perspective,” *Sex Roles*, vol. 61, no. 11–12, pp. 751–761, Dec. 2009.
[25] J. M. Cyranowski, E. Frank, E. Young, and M. K. Shear, “Adolescent Onset of the Gender Difference in Lifetime Rates of Major Depression: A Theoretical Model,” *Archives of General Psychiatry*, vol. 57, no. 1, p. 21, Jan. 2000.
[26] G. Deshpande, M. Baxi, T. Witte, and J. L. Robinson, “A Neural Basis for the Acquired Capability for Suicide,” *Frontiers in Psychiatry*, vol. 7, Aug. 2016.
[27] “Somedic, 2004. Manual for Algometer Type II. Somedic Productions, Sollentuna, Sweden.” .
[28] H. L. Urry *et al.*, “Amygdala and Ventromedial Prefrontal Cortex Are Inversely Coupled during Regulation of Negative Affect and Predict the Diurnal Pattern of Cortisol Secretion among Older Adults,” *J. Neurosci.*, vol. 26, no. 16, pp. 4415–4425, Apr. 2006.
[29] L. Spangenberg, N. Hallensleben, M. Friedrich, T. Teismann, N. D. Kapusta, and H. Glaesmer, “Dimensionality, psychometric properties and population-based norms of the German version of the Revised Acquired Capability for Suicide Scale (ACSS-FAD),” *Psychiatry Research*, vol. 238, pp. 46–52, Apr. 2016.
[30] H. Rao, M. Korczykowski, J. Pluta, A. Hoang, and J. A. Detre, “Neural correlates of voluntary and involuntary risk taking in the human brain: an fMRI Study of the Balloon Analog Risk Task (BART),” *Neuroimage*, vol. 42, no. 2, pp. 902–910, Aug. 2008.
[31] J. P. Mugler and J. R. Brookeman, “Three-dimensional magnetization-prepared rapid gradient-echo imaging (3D MP RAGE),” *Magnetic Resonance in Medicine*, vol. 15, no. 1, pp. 152–157, Jul. 1990.

[32] D. A. Feinberg *et al.*, “Multiplexed Echo Planar Imaging for Sub-Second Whole Brain FMRI and Fast Diffusion Imaging,” *PLoS ONE*, vol. 5, no. 12, p. e15710, Dec. 2010.
[33] C. L. Harenski and S. Hamann, “Neural correlates of regulating negative emotions related to moral violations,” *NeuroImage*, vol. 30, no. 1, pp. 313–324, Mar. 2006.
[34] Z. Shi and S. Han, “Transient and sustained neural responses to death-related linguistic cues,” *Social Cognitive and Affective Neuroscience*, vol. 8, no. 5, pp. 573–578, Jun. 2013.
[35] M. Lotze *et al.*, “Activation of Cortical and Cerebellar Motor Areas during Executed and Imagined Hand Movements: An fMRI Study,” *Journal of Cognitive Neuroscience*, vol. 11, no. 5, pp. 491–501, Sep. 1999.
[36] M. Weinrich, S. P. Wise, and K.-H. Mauritz, “A NEUROPHYSIOLOGICAL STUDY OF THE PREMOTOR CORTEX IN THE RHESUS MONKEY,” *Brain*, vol. 107, no. 2, pp. 385–414, 1984.